Supplementary Information

Figure S1.

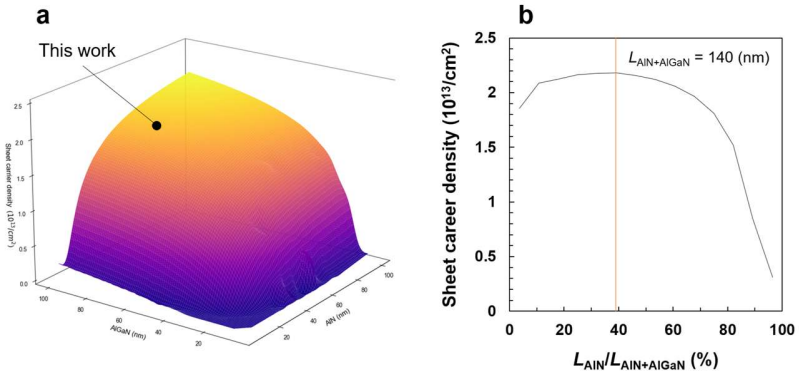

Supplementary Fig. S1 | Thickness optimization of AlN/$Al_{0.6}Ga_{0.4}N$ period. a. Calculated sheet carrier density as function of AlN and $Al_{0.6}Ga_{0.4}N$ thicknesses in single AlN/$Al_{0.6}Ga_{0.4}N$ period with AlN back barrier, obtained via self-consistent Schrödinger–Poisson simulations (FETIS 3.5). **b.** Sheet carrier density as function of thickness ratio $L_{\mathrm{AlN}}/L_{\mathrm{AlN+AlGaN}}$ for fixed total period thickness of 140 nm.

Figure S2.

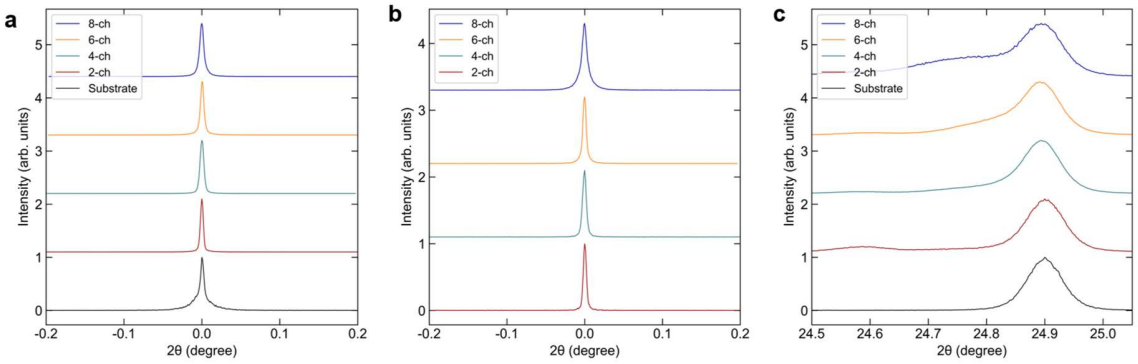

Supplementary Fig. S2 | X-ray rocking curves (XRCs) of AlN/$Al_{0.6}Ga_{0.4}N$ multichannel structures. **a.** XRCs of AlN 0002 reflection for multichannel stacks with different numbers of channels, together with AlN template. **b.** XRCs of $Al_{0.6}Ga_{0.4}N$ 0002 reflection for corresponding multichannel structures. **c.** XRCs of AlN 10−12 reflection for same set of samples. In all cases, the full widths at half maximum are comparable to those of the AlN template, indicating preserved crystalline quality across multichannel stacks.

Figure S3.

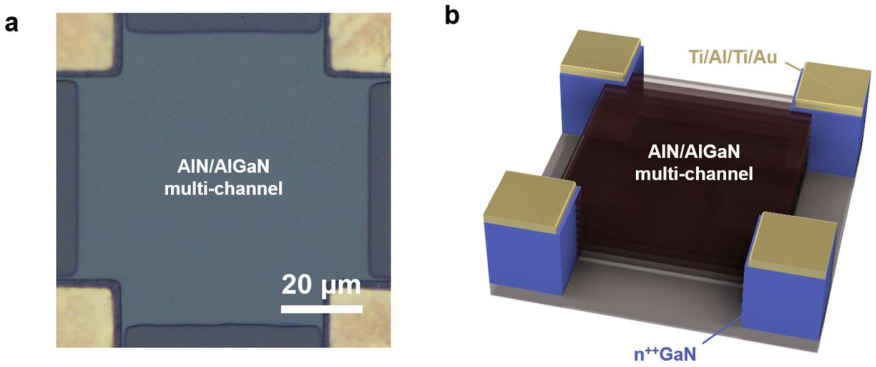

Supplementary Fig. S3 | Cloverleaf Hall-effect test structures for electrical characterization. a. Optical micrograph of cloverleaf Hall-effect test structure fabricated on AlN/$Al_{0.6}Ga_{0.4}N$ multichannel heterostructure. **b.** Schematic illustration of cloverleaf geometry used for Hall-effect measurements, enabling extraction of sheet carrier density and mobility of multichannel stacks.

Figure S4.

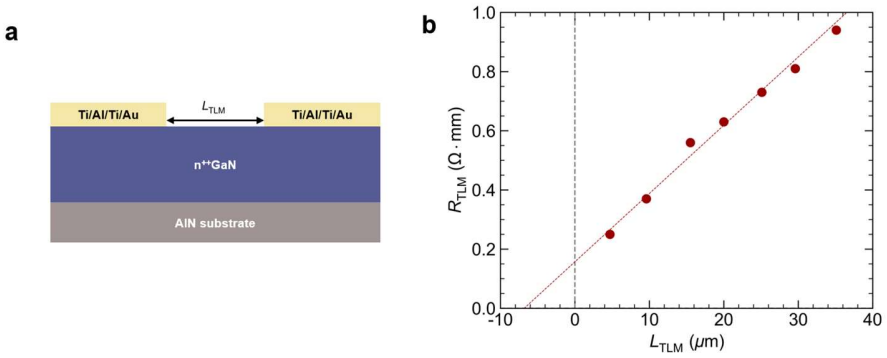

Supplementary Fig. S4 | Electrode-only transmission line method (TLM) structures for contact resistance extraction. a. Cross-sectional schematic diagram of electrode-only TLM structure consisting of Ti/Al/Ti/Au contacts formed on planar d-GaN layer grown on AlN substrate, with contact spacing L_{TLM}. **b.** Measured total resistance R_{TLM} as function of contact spacing L_{TLM}, together with linear fit used to extract contact resistance.

Figure S5.

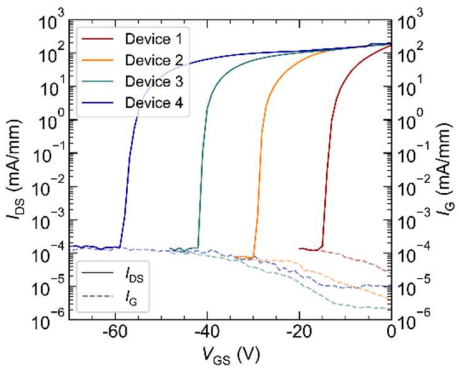

Supplementary Fig. S5 | Transfer characteristics of AlN/AlGaN multichannel HEMTs. Drain current I_{DS} (solid lines) and gate current I_{G} (dashed lines) as functions of gate voltage V_{GS} for representative devices with different nominal fin widths $L_w = 200, 400, 600, 800\ nm$.

Figure S6.

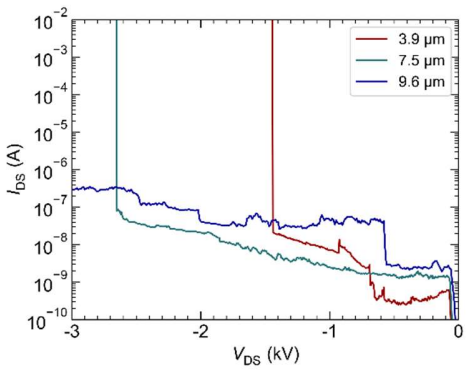

Supplementary Fig. S6 | Off-state three-terminal breakdown characteristics. Drain current I_{DS} as function of drain voltage V_{DS} measured at gate bias of V_{GS} = −15 V for devices with different gate–drain spacings L_{GD}, showing breakdown voltages up to 3 kV.

Figure S7.

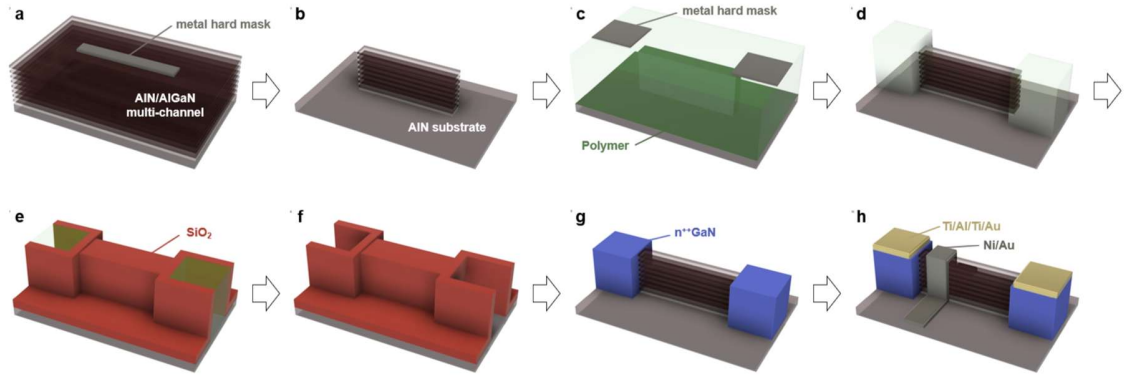

Supplementary Fig. S7 | Fabrication process flow of AlN/AlGaN multichannel HEMTs with sidewall-regrown d-GaN electrodes. a. As-grown AlN/AlGaN multichannel heterostructure with patterned metal hard mask. **b.** Fin-shaped mesa formation via dry etching. **c.** Polymer coating and definition of selective regrowth regions. **d.** Opening of sidewall regrowth windows. **e.** Deposition of SiO_2 isolation and regrowth mask. **f.** Removal of polymer. **g.** Selective regrowth of highly degenerate d-GaN on exposed sidewalls. **h.** Formation of Ti/Al/Ti/Au source–drain contacts and Ni/Au trigate electrode.

Supplementary Discussion

Contact resistance analysis

The interface-related resistance component at the regrown d-GaN/AlGaN junction (denoted as R_2 in the main text) was evaluated using Yu's TFE model for heavily doped semiconductor contacts. In this framework, the effective injection barrier at the semiconductor/semiconductor junction is represented by an effective barrier height parameter $\phi_{\mathrm{B,eff}}$. In the present implementation, we identified this parameter with the Fermi-level separation relevant to the regrown junction and set $\phi_{\mathrm{B,eff}} = \Delta E_{\mathrm{F},2}$.

In Yu's model, the specific contact resistivity ρ_C is

$$\rho_{\mathrm{C}} = \frac{k_{\mathrm{B}}^2}{qA_{\mathrm{Ri}}\sqrt{\pi(\phi_{\mathrm{bb}} + E_{\mathrm{n}})E_{00}}} \cosh\left(\frac{E_{00}}{k_{\mathrm{B}}T}\right) \sqrt{\coth\left(\frac{E_{00}}{k_{\mathrm{B}}T}\right)} \exp\left(\frac{\phi_{\mathrm{bb}} + E_n}{E_0} - \frac{E_n}{k_B T}\right), (1)$$

with

$$E_0 = E_{00}\ \coth\left(\frac{E_{00}}{k_B T}\right), (2)$$

where k_{B} is Boltzmann's constant, q is the elementary charge, A_{Ri} is the effective Richardson constant for tunneling, E_{n} is the energy separation between the relevant semiconductor band edge and the Fermi-level, E_{00} is the characteristic tunneling energy determined by the carrier concentration and dielectric properties of the semiconductor, and T is the absolute temperature. In applying the model to the regrown d-GaN/AlGaN junction, we regarded the barrier term ($\phi_{\mathrm{bb}} + E_{\mathrm{n}}$) as the effective barrier height and set ($\phi_{\mathrm{bb}} +$

$E_{\mathrm{n}}) = \phi_{\mathrm{B,eff}} = \Delta E_{\mathrm{F},2}$. The quantities A_{Ri} and E_{00} were evaluated following Yu's original formulation for degenerate semiconductors.

The composition-dependent values of the electron effective mass (m^*) and relative permittivity ε_{r} on the $Al_xGa_{1-x}N$ side were obtained from the literature. Because the transport in the present undoped Al-rich AlGaN channels is carried by polarization-induced sheet electrons, a representative effective donor concentration was introduced by converting a measured sheet density into an equivalent 3D concentration using an effective 2DEG thickness $t_{2\mathrm{DEG}}$ = 2 nm.

On the electrode side, the Fermi-level position in the degenerately doped n^{++}-GaN was estimated from the measured electron concentration (n) by assuming a 3D parabolic conduction band with BGR. The Fermi wavevector k_{F} and Fermi energy E_{F} (measured from the GaN conduction band minimum) were

$$k_{\mathrm{F}} = (3\pi^2 n)^{\frac{1}{3}}, (3)$$

$$E_{\mathrm{F}} = \frac{\hbar^2 k_{\mathrm{F}}^2}{2m_{\mathrm{e}}} - Kn^{\frac{1}{3}}, (4)$$

where $\hbar$ is the reduced Planck constant, $m_{\mathrm{e}} = 0.22m_0$ is the electron effective mass in GaN, m_0 is the free-electron mass, and $K = 2.40 \times 10^{-8}$ eV·cm is the BGR coefficient. The effective work function of the regrown d-GaN was then obtained by combining the Fermi-level position with the GaN electron affinity χ = 3.1 eV. For the present PSD-grown d-GaN films with $n \approx 3.0 \times 10^{20}$ cm^{-3}, this procedure yields $\phi_m \approx 2.52$ eV.

Because the transfer-length relation $L_{\mathrm{T}} = \sqrt{\rho_C / R_{\mathrm{sh}}}$ assumes a continuous conductive sheet under an overlapping contact, it was not used to convert ρ_C into a width-normalized interface resistance for the present sidewall-injection geometry. Instead, for the single-channel devices only, ρ_C was converted into a width-normalized model value by assuming that current is injected into a 2DEG layer of effective thickness $t_{\mathrm{2DEG}} = 2\ \mathrm{nm}$ at the regrown sidewall interface. With an effective contact area per unit width $A_{\mathrm{eff}}/W = t_{\mathrm{2DEG}}$, the model interface resistance was obtained as $R_{2,\mathrm{model}} = \rho_C/(A_{\mathrm{eff}}/W) = \rho_C/t_{\mathrm{2DEG}}$ and converted into ohm-millimeters using consistent unit conversion between centimeters and millimeters. The resulting $R_{2,\mathrm{model}}$ values were compared with R_2 extracted from TLM measurements of the corresponding single-channel devices.